THESIS

ESTIMATING FIFTY-TWO YEARS OF GROUNDWATER LEVELS IN DIFFERENT AQUIFER LAYERS IN THE SOUTHERN SAN JOAQUIN VALLEY, CALIFORNIA

Submitted by

Susmita Pant

Department of Civil and Environmental Engineering

In partial fulfillment of requirements

For the Degree of Master of Science

Colorado State University

Fort Collins, Colorado

Summer 2025

Master's Committee:

Advisor: Ryan Smith

Ryan Bailey
Douglas P. Frankell

ABSTRACT

ESTIMATING FIFTY-TWO YEARS OF GROUNDWATER LEVELS IN DIFFERENT AQUIFER LAYERS IN THE SOUTHERN SAN JOAQUIN VALLEY, CALIFORNIA

Over the past century, California's San Joaquin Valley has faced dramatic groundwater level depletion. Significant spatial and temporal gaps in the records, unreliable measurements, and unknown depths to which most wells are drilled, hinder effective groundwater monitoring in the region. This study presents a novel method, which integrates a time series technique called Small Baseline subset (SBAS) with kriging to estimate yearly changes in groundwater levels, as well as total absolute head from 1971 to 2023 in the Southern San Joaquin Valley across two distinct aquifer layers – one shallow (mostly unconfined) aquifer and one deep (confined) aquifer. Firstly, 1,197 wells with known depths based on the depth of an extensive confining layer, the Corcoran Clay, were classified. Further, 348 wells with unknown depths, which were within the clay boundary, were categorized by examining the correlations and differences in the average yearly fluctuations of groundwater levels with the 1197 wells. Out of these 348 wells, 215 wells belonged to confined and 133 were assigned to mostly unconfined aquifers. 3,039 wells were outside the Corcoran Clay Layer, which were classified as mostly unconfined because they exhibited a similar distribution of seasonal groundwater fluctuations to the mostly unconfined group. For each of the aquifers, we used ordinary kriging to estimate groundwater level change over specific intervals (every 1, 2, 3, 4, 5, 6, 7, and 8 years for all wells with available data) across the study area. Using a system of linear equations, we then solved for the yearly change in groundwater level from 1971 to 2023. The mean reduction in groundwater level from 1971 to 2023 was observed to be 16 m for

mostly unconfined aquifers and 23 m for confined aquifers. The groundwater levels declined sharply for both aquifers during drought periods because of the increased reliance on groundwater for irrigation. In addition, we used our predicted groundwater level data to estimate that a total of 19.8 km^3 (0.7 to 1.9% of the total freshwater groundwater storage in the Central Valley) water was lost from the study area between 2015-2023, with most of the storage loss (80%) coming from mostly unconfined aquifers, followed by compaction of aquifer matrix (20%).

TABLE OF CONTENTS

LIST OF TABLES

LIST OF FIGURES

1. INTRODUCTION

1.1 Background

With approximately 99% of the earth's liquid freshwater, groundwater holds a significant portion of the planet's freshwater reserves (United Nations, 2022). It is estimated that around 2.5 billion people in the world rely on it to meet their basic daily water demands (Akhter et al., 2023). However, there has been rapid groundwater decline in many places of the world such as different regions of Iran, China, United States, Bangladesh, and India (Hasan et al., 2023). Such overexploitation of groundwater has not only resulted in depletion of these resources but has also given rise to problems such as arsenic contamination, saltwater intrusion, and land subsidence (Hasan et al., 2023; Jasechko et al., 2024; Jia et al., 2020; Smith et al., 2018).

In the United States, California's San Joaquin Valley, one of the world's most productive agricultural regions, relies heavily on groundwater for irrigation (Faunt et al., 2016; Galloway & Riley, 1999). Due to this, the region has some of the most heavily pumped aquifers in the country, causing a decline of up to 60 m in groundwater levels over the past century, resulting in subsidence of up to 9 m from 1925 to 1970 (Poland et al., 1975). Another study by Ojha et al., (2019) reported that the total volume of water lost from October 2011 to September 2015 was observed to be 24.2 ± 9.3 km^3 in the valley, with 0.4 to 3.25% of the aquifer system storage capacity permanently lost during this drought period. According to Liu et al. (2022), the Tulare Basin (covering southern part of the San Joaquin Valley) had a total volume change of 16.1 ± 0.3 km^3 and an annual groundwater volume change rate of 0.88 ± 0.06 km^3/yr between September 2003 and December 2021, with the agriculture sector accounting for most of the water demand. Furthermore, during the 2012-2016 drought, of the 2,600

households reliant on wells across California, who reported water shortages, nearly eighty percent were situated in the San Joaquin Valley (Hanak et al., 2020). In many locations, the average annual decline rate has been more than 0.76 meters (Bland, 2023). Thus, monitoring groundwater levels in the area is crucial for tracking groundwater trends, understanding aquifer dynamics over time, and developing numerical groundwater models which will ultimately help in groundwater management (Peterson & Western, 2018).

Although there is a dense network of wells in the area, the groundwater level records have large temporal and spatial gaps. There are also multiple aquifers in the San Joaquin Valley, so direct interpolation of water levels without this consideration may lead to errors (Levy et al., 2021). These records must be filled accurately and reliably to understand the effects of groundwater availability and withdrawals, change in water quality, land subsidence and surface water-groundwater interaction (Taylor & Alley, 2001).

Various methods have been developed for groundwater level interpolation. Among these, kriging is one of the most often used geostatistical approaches. It is extensively used to estimate various groundwater parameters as it provides a map of both the interpolation and uncertainty associated with the interpolated data (Evans et al., 2020). Júnez-Ferreira et al., (2023) used spatial-temporal kriging to estimate groundwater levels in the Southern Basin of the Mexico Aquifers from 2002 to 2007. A similar study done by Ruybal et al., (2019) developed interpolated maps of groundwater levels for 324 months between 1990 to 2016, using spatiotemporal kriging in the Arapahoe Aquifer. Similarly, Masoudi et al., (2024) used ordinary kriging and universal kriging to map the water table in California using groundwater level data from 160 piezometers. Likewise, different machine learning models have also been widely used to predict aquifer depth across different aquifers of Iran, the United States, Turkey, China and India (Tao et al., 2022). Furthermore,

combined use of Kriging and Multi Linear Regression (MLR) has also proved to be efficient in groundwater estimation (Evans et al., 2020; Levy et al., 2021). Evans et al., (2020) developed a groundwater mapping tool to estimate water levels in the Cedar Valley Aquifer, Utah, from 1985 to 2015. For this, MLR was used to fill in the temporal gaps using the groundwater level data of the five most correlated wells. Then, kriging was applied to fill in the spatial gaps. A similar approach was used by Levy et al., (2021) for groundwater level estimation using annual time steps from 1990 to 2018 for the California's Central Valley Aquifer.

The efficiency of methods like kriging, machine learning and regression models is highly dependent on the volume and quality of the data. Often, groundwater level records can have discrepancies due to the presence of perched aquifers, measurement errors, technical problems at the observation site, and local anthropogenic impacts (British Geological Survey, n.d.; Retike et al., 2022; Snyder, 2008). This issue is also observed within the San Joaquin Valley. Moreover, numerous wells are drilled close to each other, which can lead to cone of depression effects from nearby pumping wells, which cause the measured observation to deviate from the regional groundwater table. Previous studies have also reported that a lack of regular and good quality water level data has presented challenges in the groundwater management of the San Joaquin Valley (Lees & Knight, 2023; Pradhan et al., 2024). In addition to that, wells across different aquifers in the valley have distinct patterns and seasonal fluctuation in head measurements (Lees et al., 2022). As a result, estimation and interpolation of the head measurements could be inaccurate and result in error, if the available wells are not classified to the proper aquifer. In the study area, the depths to which most of the wells are drilled to is unknown, hindering the identification of the aquifers to which they belong.

One of the severe effects of excessive groundwater extraction is land subsidence, which can be monitored via remote sensing, spirit-level surveys, and the Global Positioning System (GPS). In remote sensing, Interferometric Synthetic Aperture Radar (InSAR) is widely used to measure surface deformation at millimeters to centimeters level accuracy (Smith & Knight, 2019). It is based on measuring the phase difference between two radar images taken at two different times but from the same location (also called as interferograms). One widely used technique in InSAR is the Small Baseline Subset (SBAS) approach. The approach is used to process time series of deformation from InSAR data by combining information from multiple overlapping time periods (multiple interferograms) (Berardino et al., 2002). This method has been effective in removing noise, eliminating temporal and spatial decorrelation and generating accurate time-series of deformation (Li et al., 2022; Yu et al., 2024). Therefore, it could be an appropriate approach to eliminate errors from the groundwater level data. As a matter of fact, Smith, (2023) used it to estimate yearly head change over an 80-year time span using periodic head measurements from different wells in the valley and found out that the method effectively tracks the regionally average head changes.

This research aims to develop dense spatiotemporal estimates of groundwater levels including absolute groundwater head from 1971 to 2023 in the Southern San Joaquin Valley by tackling the issue of the sparse datasets in the noisy settings. For this, we first classified the wells in the southern San Joaquin Valley into the appropriate shallow (mostly unconfined) or deep (confined) aquifers using an automated approach that leveraged correlation to nearby wells, and the average yearly change in groundwater levels. We then integrated SBAS with kriging to estimate yearly change in groundwater levels from 1971 to 2023 in the study area, with the objective of removing noise

from the data. Finally, we also estimated the approximate groundwater storage loss from the aquifer from 2015 to 2023 for the study area.

1.2 Study Area

The study area is the major portion of the Tulare Basin that intersects the Central Valley and covers roughly the southern two thirds of the San Joaquin Valley, California (Figure 1). Subsidence due to high groundwater level decline was centered around the western portion of the San Joaquin Valley from the 1940s to the 1970s. The 1968 aqueduct construction and years with heavy precipitation reduced groundwater demand in this region after the 1970s. However, in the southern portion, the head rapidly dropped below the pre-consolidation head due to droughts in the 1990s. This caused the subsidence to shift to the southern portion from the western part of the valley after the 2000s (Smith, 2023).

Geographically, the area is bounded by the Sierra Nevada in the east and coastal ranges in the West. Coarse oxidized continental and alluvial sediments, including marine rock of Pre-Tertiary age from the Coastal Ranges, predominate on the western side of the valley, whereas alluvial deposits prevail in the southern region. Furthermore, reduced continental and alluvial fan deposits from the Sierra Nevada is abundant in the eastern side of the valley (Croft, 1972). In addition, lacustrine and marsh deposits are more prevalent in areas such as Buena Vista, Kern, and Tulare Lake Beds (Page, 1986). Extending over a major part of the study area, along the western side, is the laterally extensive lacustrine clay called the Corcoran Clay Layer, which has thickness of up to 61 m and divides the upper and lower aquifers (U.S. Geological Survey, 2023). The Tulare Lake Bed and adjacent area have the thickest and most widespread clay deposit, with depths reaching up to 1,097 m (Page, 1986). In most of the study area, the fine-grained sediments are

interbedded with the coarse-grained sediments, especially in Tulare and Kern County (Faunt, 2009; Page, 1986). Studies have shown that numerous lenticular clay units of varying thickness are distributed throughout the upper and lower aquifers (Lees & Knight, 2023; Smith et al., 2017). As a result, aquifers are not fully unconfined in nature (hereafter called mostly unconfined) in the upper aquifer (Figure 2; Figure 3).

The Tulare Basin has over 15,000 km^2 of irrigated agricultural land with the total sum of agricultural products of over $26 billion in 2021 in Kern, Fresno, Tulare and Kings County (California Department of Food and Agriculture, 2022; Mayzelle et al., 2015). Thus, the study area is a major global agricultural hub with main crops ranging from grains, grapes, alfalfa, almonds, pistachios, cotton and corn (California Water Library, 2025; USGS California Water Science Center, 2025). However, 4,307 wells have gone dry in the basin, which is over 77% of all wells that have gone dry in California (Dry Well Reporting System, 2025; Visser et al., 2024). As a result, it is important to understand the groundwater dynamics in the region.

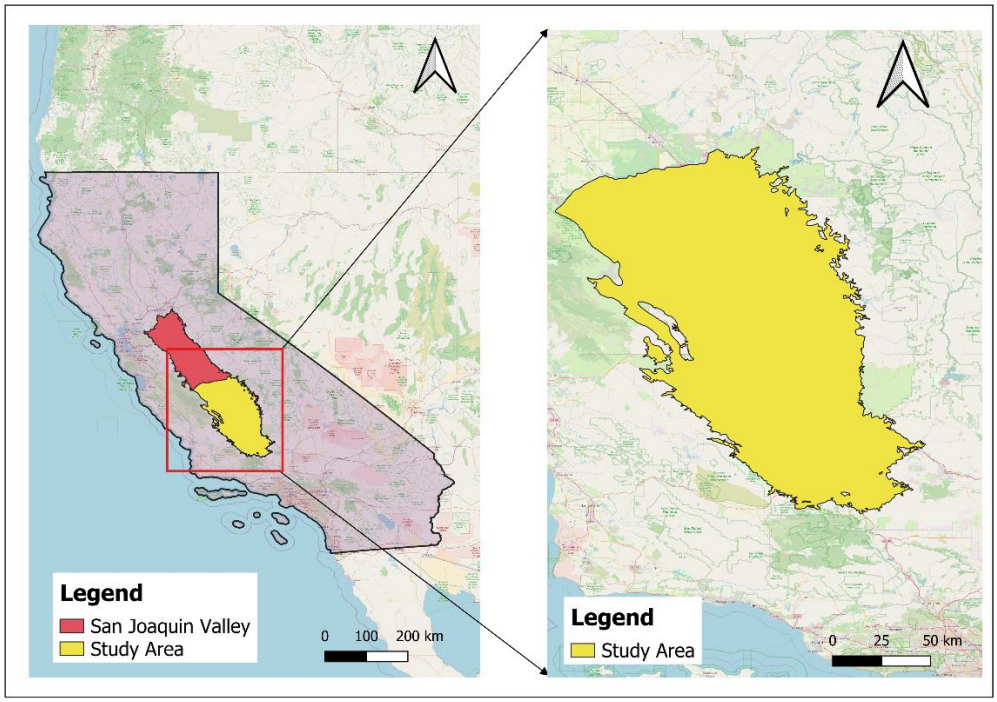

Figure 1. Map of the Study Area

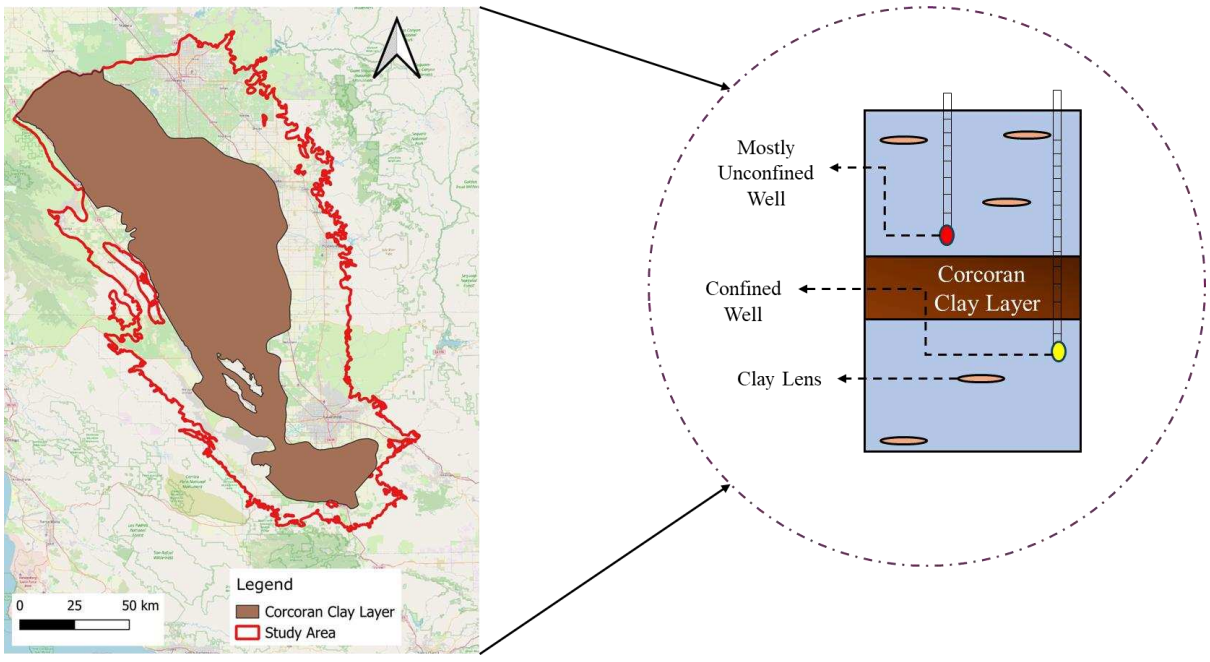

(a) (b)

Figure 2. Extent of Corcoran Clay in the study area (a), with simplified overview of the subsurface geology showing the upper and lower aquifer layer (b)

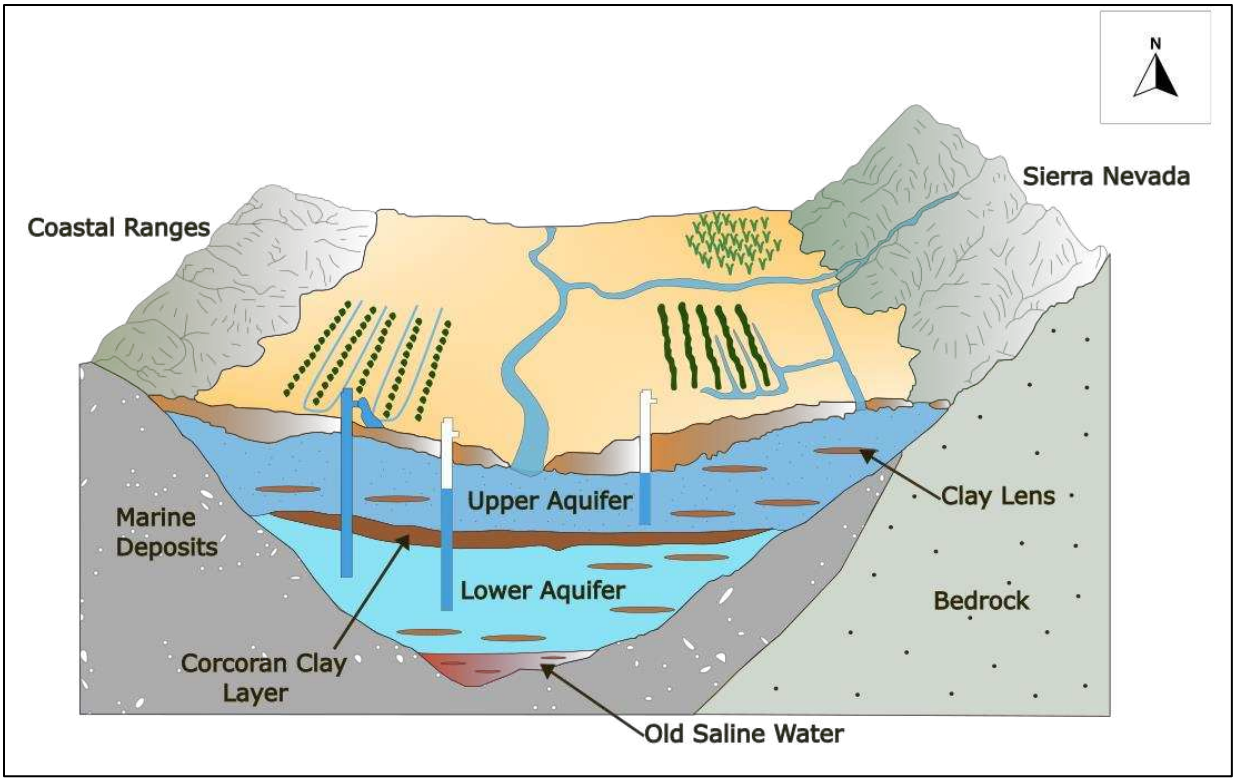

Figure 3. Cross Section of the study area showing the surrounding geology, upper aquifer, lower aquifer as well as main confining unit (Corcoran Clay and clay lens) (modified from Faunt et al., 2009).

2. MATERIALS AND METHODS

2.1 Data Collection and Filtering

Groundwater level records (Depth to groundwater) from the wells, present in our study area between 1900 and 2023, were collected from the California Department of Water Resources (California Natural Resources Agency Open Data, 2025). As pumping activities are typically higher during the fall season, leading to the formation of cones of depression around wells (Smith, 2023), only data of spring season from January 1 to April 1 were considered. The dataset was further refined by removing depth to groundwater levels greater than 305 m because they were anomalously high. In addition to that, well data with water levels above the land surface, i.e., depth to groundwater less than 0 were also removed, because they were unusually low, and no artesian wells were considered in the study. Finally, the yearly groundwater level for each well was derived from the average value of all remaining spring measurements for each year.

2.2 Classification of Wells

2.2.1 Classification Based on Depth of the Corcoran Clay Layer

Initially, the wells that had depth data, and were inside the Corcoran Clay Layer were categorized. For this, depths of the drilled wells were compared with the Corcoran Clay Layer thickness to classify these wells in their respective aquifers. A contour map representing the depth of the Corcoran Clay layer was obtained from California Natural Resources Agency Open Data (Page, 1986; U.S. Geological Survey., 2023). A Triangulated Irregular Network (TIN) was generated and rasterized from the contour map. Out of the 8,041 wells present in the study area, 1,197 wells had well depth data. These were clipped on the rasterized Corcoran Clay depth layer and then categorized. If the depth of the well was greater than the depth of the top of the Corcoran

clay layer, the well was classified as belonging to the deep (confined) aquifer. In the other case, it was identified as belonging to the shallow (mostly unconfined) aquifer.

2.2.2 Classification of the Wells with Unknown Depth inside the Corcoran Clay Layer

Secondly, wells that were inside the Corcoran Clay layer extent were grouped. This was done by comparing to the wells that were initially classified in section 2.2.1. For each of the unclassified wells, the 40 nearest classified wells were identified. The Pearson Correlation Coefficient (*r*-value) as well as the mean yearly change in groundwater levels was calculated when a minimum of 10 common years of groundwater level data were available for both the given unclassified well and classified wells. The absolute difference in mean annual change was computed for each unclassified well vs each classified well. The unknown well's mean correlation coefficient, as well as the mean absolute difference in yearly water level change was determined with both the confined and mostly unconfined groups. To avoid the classifying the wells that are similar to both the confined and mostly unconfined, if screened over both the intervals, we only classified a well if the average *r-value* of one of the categories is at least 0.2 times higher than the average *r-value* of the other category. We expected that if the well was in one of the categories, there would be a high correlation with that category and a very low absolute difference in the annual change in groundwater levels. Accordingly, the well was categorized based on the greatest correlation value and the lowest yearly change difference if the mean correlation was more than 0.75 and the difference in the annual change in water levels was less than 3 meters. The process continued until the maximum number of wells were classified. The classified wells that had been determined in each iteration were also included for the use in the following one.

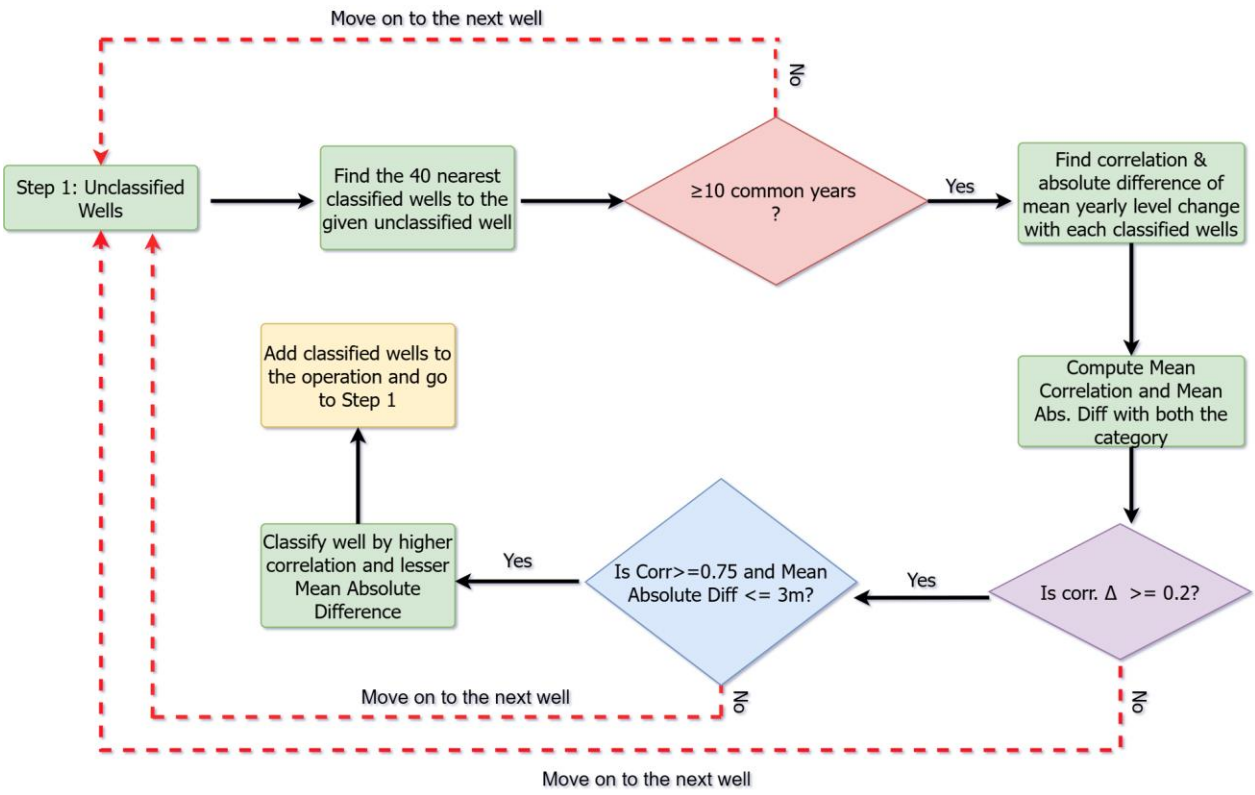

Figure 4. Schematic showing how a well is classified using the Correlation and yearly depth change Analysis

2.2.3 Classification of the Wells outside the Corcoran Clay Extent

Typically, in the spring season, groundwater levels rise because of the increased recharge from the snowmelt and precipitation, while in the fall season groundwater levels reduce drastically because of the water extraction for irrigation and limited rainfall. Confined and mostly unconfined aquifers respond differently to seasonal variations and pumping-induced changes in groundwater levels. This results from variations in the aquifer's water addition or release mechanism, which is quantified by "storativity,"- the amount of water added or released per unit surface area per unit change in hydraulic head. In mostly unconfined aquifers, the key mechanism of water storage change is the gravity drainage which is defined by the “specific yield”, whose value ranges from 0.01 to 0.30 (Freeze & Cherry, 1979). Confined aquifers are bounded by low permeability

confining layers and are under high pressure, resulting in a distinct mechanism for water storage. Compression or expansion of the aquifer system/water adds or releases water in these aquifers. The storativity value in these aquifers is very low ranging from 0.005 to 0.0005 (Freeze & Cherry, 1979). As a result, even with small amount of water released or added to the system, the head change is high. In contrast, high value of specific yield in mostly unconfined aquifers result in moderate change in groundwater levels even with large amount of water input or loss. Thus, we leveraged this property to classify the wells in their respective aquifers.

Wells outside the Corcoran Clay layer extent were categorized by comparing seasonal changes in groundwater levels to classified wells inside the clay layer. The maximum depth to groundwater levels were evaluated for the fall season (August to November) and the minimum depth to groundwater levels for the spring season (January to May) for each well for each year. The difference between the spring minimum and fall maximum was computed for all classified wells within the Corcoran Clay layer extent (with known and unknown depth data) and wells outside the Corcoran Clay layer area for each year. A box plot showing the distribution of the maximum seasonal change was generated, including the spread and central tendency. Wells outside of the clay were grouped based on the distribution of the maximum seasonal change pattern observed in the box plot.

2.3 Estimation of Changes in Groundwater Level

Yearly change in groundwater levels from 1971 to 2023 was estimated by integrating Kriging with an InSAR time series technique called SBAS for both the shallow (mostly unconfined) and deep (confined aquifer) layers. The process involved applying kriging to interpolate changes in groundwater levels at various time intervals across the study area and then implementing the SBAS technique to find the annual change in groundwater levels.

2.3.1 Kriging

Kriging is a geostatistical interpolation tool that helps to predict the values at unsampled locations using the spatial correlations in the available datasets. It is a multi-step process that includes determining the semi-variance between the points, fitting the variogram model, computing the weights from the fitted variogram model, and lastly interpolating values at the given point from the calculated weights.

From the available yearly depth to groundwater table data, groundwater level changes at each well were calculated for every 1,2,3,4,5,6,7, and 8 years from 1971 to 2023. Ordinary Kriging with spherical variogram was applied to estimate the groundwater level difference across the study area for each of these intervals. The primary assumption for Ordinary Kriging is that the data points exhibit stationarity (i.e., stationarity in the context of kriging implies that the variogram is valid across the study space) and isotropy. While there is natural variation in hydrogeology across the study area, previous work has indicated that this assumption is valid for the San Joaquin Valley (Faunt et al., 2009). In addition to that, we also assumed that the variogram was constant throughout the study period, i.e. the spatial correlation of the groundwater levels does not change significantly over time. Therefore, the median values for the sill, nugget, and range were obtained for each of the intervals, and the variogram was constructed using the median of these values, which were then applied to every interval range. Thus, kriged raster datasets representing changes in groundwater levels every 1, 2, 3,4, 5, 6, 7, and 8 years were generated for each of the aquifer layers throughout the study region.

2.3.2 Application of the SBAS Technique

Yearly changes in groundwater levels from 1971 to 2023 were computed using the Small Baseline Subset (SBAS) approach SBAS (Berardino et al., 2002). Kriged surfaces of the groundwater level

change for 1 to 8 years were used to solve for the yearly change in water levels using the system of linear equations to determine the best fit. The following relation is used at each cell of our kriged rasters to define the system of linear equations:

$$\boldsymbol{Ax=b} \tag{1}$$

Here, **'A'** is an **mxn** matrix containing either 0 and 1 because we are solving for annual change in groundwater levels (1 year). Here, ***'m'*** rows represent the number of intervals and ***'n'*** represents the annual intervals. **'x'** is the unknown matrix with ***'nx1'*** order, and **'B'** is the matrix with **'mx1'** order.

A simplified example of the system of equations to estimate annual change in groundwater level groundwater level difference for 1,2, 3, and 4 years from 1971 to 1975 is shown below:

$$\begin{bmatrix} 1 & 0 & 0 & 0 \\ 1 & 1 & 0 & 0 \\ 1 & 1 & 1 & 0 \\ 1 & 1 & 1 & 1 \\ 0 & 1 & 0 & 0 \\ 0 & 1 & 1 & 0 \\ 0 & 1 & 1 & 1 \\ 0 & 0 & 1 & 0 \\ 0 & 0 & 1 & 1 \\ 0 & 0 & 0 & 1 \end{bmatrix} \begin{bmatrix} \Delta h_{1971-1972} \\ \Delta h_{1972-1973} \\ \Delta h_{1973-1974} \\ \Delta h_{1974-1975} \end{bmatrix} = \begin{bmatrix} \Delta h_{1971-1972} \\ \Delta h_{1971-1973} \\ \Delta h_{1971-1974} \\ \Delta h_{1971-1975} \\ \Delta h_{1972-1973} \\ \Delta h_{1972-1974} \\ \Delta h_{1972-1975} \\ \Delta h_{1973-1974} \\ \Delta h_{1973-1975} \\ \Delta h_{1974-1975} \end{bmatrix} \tag{2}$$

In the above demonstration, the first matrix is ***'A'***, the following second matrix is ***'x'*** and the matrix to the right-hand side of the '=' is ***'b'***. Here, a system of 10 equations is used to solve the unknown yearly change in head for 4 years. In this study, 388 sets of linear equations were used to solve for the unknown yearly change in head for 52 years (from 1971 to 2023), for each pixel of the kriged raster, using change in head data from 1, 2, 3,4 up to 8-year intervals.

Finally, kriging with spherical variogram was performed to interpolate absolute head for the year 1971 throughout the study area. Yearly groundwater levels change was added to this kriged surface to estimate absolute head from 1972 to 2023.

2.4 Estimation of Storage Loss from 2015 to 2023

Approximate yearly storage loss from 2015 to 2023 was calculated, based on the storativity value in the respective aquifer layer and the yearly groundwater level change rasters produced in this study. In the mostly unconfined portion of the aquifer, the storativity can be considered the same as specific yield (Freeze & Cherry, 1979; Stevens et al., 2025). The associated groundwater storage loss from the mostly unconfined portion ($\Delta V_{mostly\ unconfined}$) was obtained by multiplying the specific yield ($\boldsymbol{S_y}$), with area of each pixel ($\boldsymbol{A_{pixel}}$) and the yearly groundwater level change ($\boldsymbol{\Delta h}$) in the respective pixel. This can be represented by:

$$\Delta V_{mostly\ unconfined} = S_y \times \Delta h \times A_{pixel} \quad (3)$$

Specific Yield ($\boldsymbol{S_y}$), values for each pixel of the study area was obtained from the Central Valley Hydrological Model (CVHM) (Faunt et al., 2009).

In the confined aquifer system, aquifer depletion is caused by the compression of aquifer materials (coarse and fine-grained confining layers/clay lens) and the expansion of water. Specific Storage ($\boldsymbol{S_s}$) , which is the volume of water that can be lost/produced per unit volume of the aquifer system per unit change in head, because of the compression or expansion of the aquifer matrix or water, is used to define this relation (Smith et al., 2017). $\boldsymbol{S_s}$ can be defined by the following equation:

$$S_s = \rho_w g \times (\alpha + \eta\beta) \quad (4)$$

In the given equation, ρ_w is the density of water, g is the acceleration due to gravity, α is the compressibility of the aquifer, η is the porosity, and β is the compressibility of the water. The equation has two components, $\boldsymbol{S_s = S_{SK} + S_{SW}}$ where, $\boldsymbol{S_{SK}} = \rho_w g\alpha$ is the specific storage of

aquifer matrix (coarse grained and fine-grained materials and $\boldsymbol{S_{SW} = \rho_w g \eta \beta}$ is the specific storage of the water. Hence, the amount of storage decline can be obtained from the equation below:

$$\Delta V_{confined} = S_{SK} \times b \times \Delta h_{matrix} \times A_{pixel} + S_{SW} \times b \times \Delta h_{confined} \times A_{pixel} \quad (5)$$

Here, b is the original thickness of the aquifer, Δh_{matrix} is the yearly groundwater level changes in the matrix, and $\Delta h_{confined}$ is the annual groundwater level changes in the confined aquifer. $\boldsymbol{S_{SK}}$, which is the specific storage of aquifer matrix (coarse grained and fine-grained materials), is also referred to as the skeletal specific storage, and can be represented by the relation between $\boldsymbol{\Delta b}$ (change in thickness of the compacting material), $\boldsymbol{\Delta h_{matrix}}$ and $\boldsymbol{b}$ denoted by:

$$S_{SK} = \frac{\Delta b}{\Delta h_{matrix} \times b} \quad (6)$$

Thus, the storage loss from the confined portion is obtained by the given relation

$$\Delta V_{confined} = \Delta b \times A_{pixel} + S_{SW} \times b \times \Delta h_{confined} \times A_{pixel} \quad (7)$$

Ground deformation (Δb) data was obtained from remotely sensed InSAR from the California Department of Water Resource, which is available online at (https://data.cnra.ca.gov/dataset/tre-altamira-insar-subsidence). TRE Altamira processed the InSAR data using hundreds of the interferograms over a long period of time via SBAS. Line of Slight (LOS) ground displacement data obtained from Sentinel-1 satellite imagery is used. These LOS measurements are calibrated against the GNSS stations to align with an absolute reference frame (Tre Altamira, 2024; Neely et al., 2024).

The InSAR subsidence data were acquired from 2015 to 2023, covering progressive time intervals, that included 2015-2016, 2015-2017 and subsequent years. To calculate the overall storage loss from the compression of the aquifer matrix, the deformation value at each pixel was

multiplied by the pixel's area and summed up. For the thickness of the aquifer ($\boldsymbol{b}$), the total thickness of 549 m from the CVHM model was used as an upper bound (California Department of Water Resources (DWR), 2016). To account for the storage loss because of the expansion of the water, specific storage value ($\boldsymbol{S_{SW}}$) = 4.59×10^{-6} m^{-1} obtained from the CVHM model (Faunt et al., 2009) was used, which was multiplied by the groundwater level change, assumed $\boldsymbol{b}$, and the area of the pixel. Give the very low S_{SW}, the resulting impact should also be minimal even for the maximum thickness of the aquifer.

3. RESULTS AND DISCUSSIONS

3.1 Classification of the Wells

1,197 wells present in the study area had information regarding depth to which they were drilled; 275 of these wells were classified as belonging to the shallow-mostly unconfined aquifers, whereas 922 wells were classified to deep-confined aquifers. While the drilled depth of the confined wells ranged from 76 m to 914 m with an average depth of 368, the depth of the mostly unconfined wells ranged from 0 to 229 m with a mean depth of 97 m. By examining the correlations and differences in the average yearly fluctuations of groundwater levels, using these wells, a total of 348 wells with unknown depth data that were inside the Corcoran clay layer were classified. Out of these 348 wells, 215 wells belonged to confined and 133 were assigned to mostly unconfined aquifers. Based on the assessment of the maximum seasonal change in groundwater levels across the classified well groups, confined wells exhibited greater variability, and wider interquartile ranges along with higher medians, in comparison to the mostly unconfined wells (Figure 5). This is consistent with the expectation that there is larger seasonal change in confined aquifers than the mostly unconfined (Lees et al., 2022). 3,039 wells were outside the Corcoran Clay Layer, which were classified as mostly unconfined because they exhibited similar distribution of the seasonal groundwater fluctuation to that group, and they are outside of the main confining unit area. Most of the unconfined wells were clustered towards the eastern side of the valley (Figure 6). This pattern can also be attributed to the presence of alluvial fan deposits that predominantly have coarse grained sediments from the Sierra Nevada Range on the eastern side of the valley, which becomes fine grained towards the axis of the valley (Phillips et al., 2007).

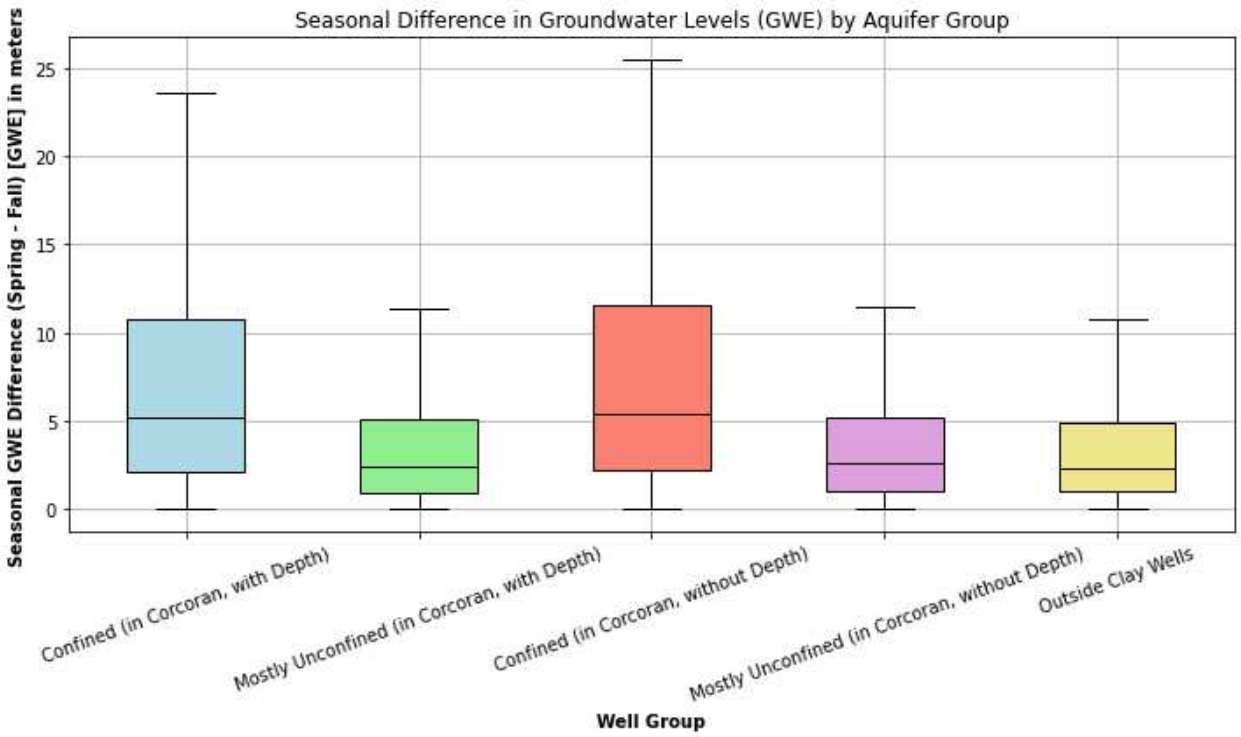

Figure 5. Seasonal differences in the groundwater levels across different groups

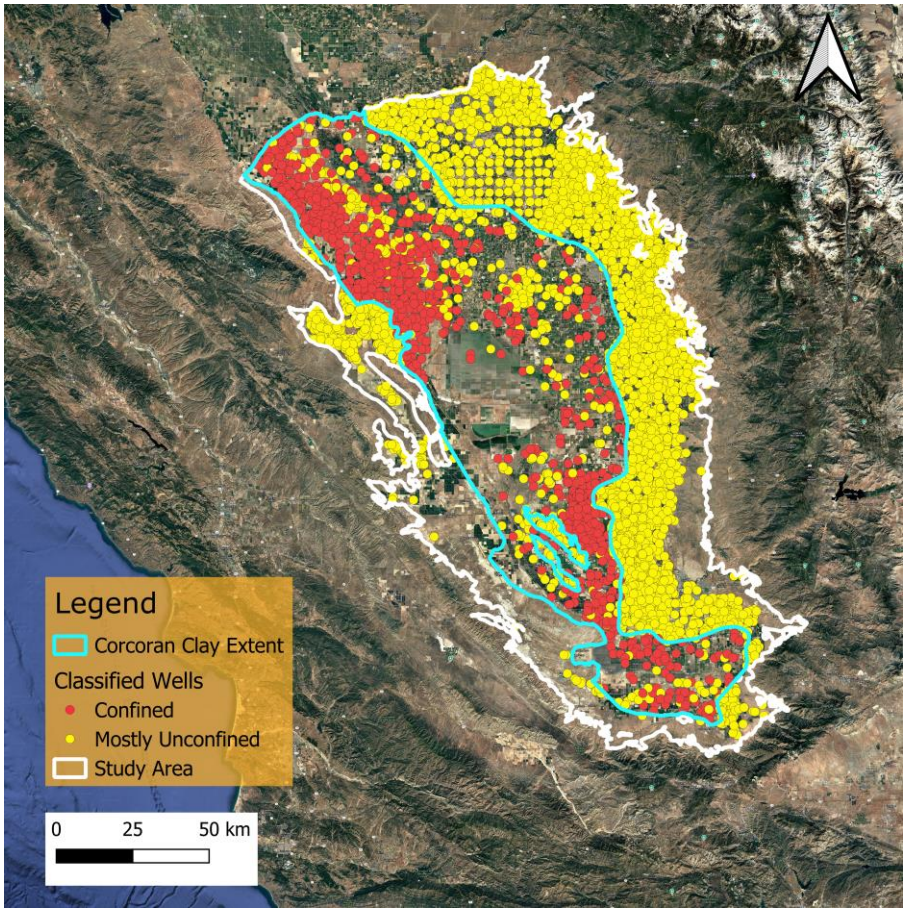

Figure 6. Classification of the Drilled Wells in the Valley

3.2 Validation of the Classified Wells

For validation of the wells, a K-Fold Cross validation technique with 5 folds was used. Wells which had depth to which they were drilled were divided into 5 subset/folds. For each iteration 4 of the 5 folds were divided into training datasets. We added classified wells that did not have drilled depth data and were inside the Corcoran clay layer to the training dataset. Moreover, mostly unconfined wells outside of the clay extent were also included in the analysis. Wells in the "test" fold were categorized based on the combined correlation/mean yearly change in water levels analysis as described in Section 2.2.2. For the wells that were classified, accuracy score i.e., $\left(\frac{Number\ of\ correct\ predictions}{Total\ number\ of\ predictions}\right)$ for each of the "test" folds were calculated. The average accuracy score from validation of each of the folds was computed as 0.88. Thus, the results indicated that

the method was effective in classifying the wells. However, classification uncertainties can be caused by multiple factors, including perforation intervals that span both confined and mostly unconfined sections, well perforation inside clay lenses, and the impact of cones of depression from the pumped nearby wells.

3.3 Groundwater Level Changes from 1971-2023

Cumulative change in groundwater levels in both the aquifers, in the span of 52 years, was discernibly different (Figure 7). In majority of the study area the groundwater levels decreased. From 1971 to 2023, cumulative groundwater level changes in the mostly unconfined aquifer ranged from 1.8 meters rise to 47.8 meters fall. In the case of confined aquifers, it changed from 6.6 meters rise to a fall of 53.3 meters in the same time span. In both the aquifer layers, the western side (near Los Banos) area showed relatively lower groundwater level changes throughout the 52-year time periods compared to the southern portion. This is because of the shift of the aquifer stress from the western to the southern part after 1970 (Smith, 2023). The Central South portion of the valley showed the highest reduction in groundwater level changes, likely driven by the extensive presence of irrigation dependent agricultural land in this area. The sides of the valley showed less fall in groundwater levels change, compared to this portion, due to faster recharge and comparatively higher elevation. We observed that the fall of the groundwater levels was greater in the confined system compared to the unconfined system. This is because of the longer recharge time for the deeper confined aquifers. Furthermore, the confined aquifer's storativity value is significantly lower than the mostly unconfined aquifer's, which results in a slower and lower recharge response. Any confined aquifer will have some confining layer that blocks recharge. So, slower recharge is further catalyzed by the presence of thick Corcoran Clay layer between the upper and lower aquifer. For the mostly unconfined aquifers, portion at the central-western side

showed a patch of high recharge area. Interpolation in this region shows a high degree of uncertainty, largely resulting from artifacts in the kriging process caused by the limited availability of well data.

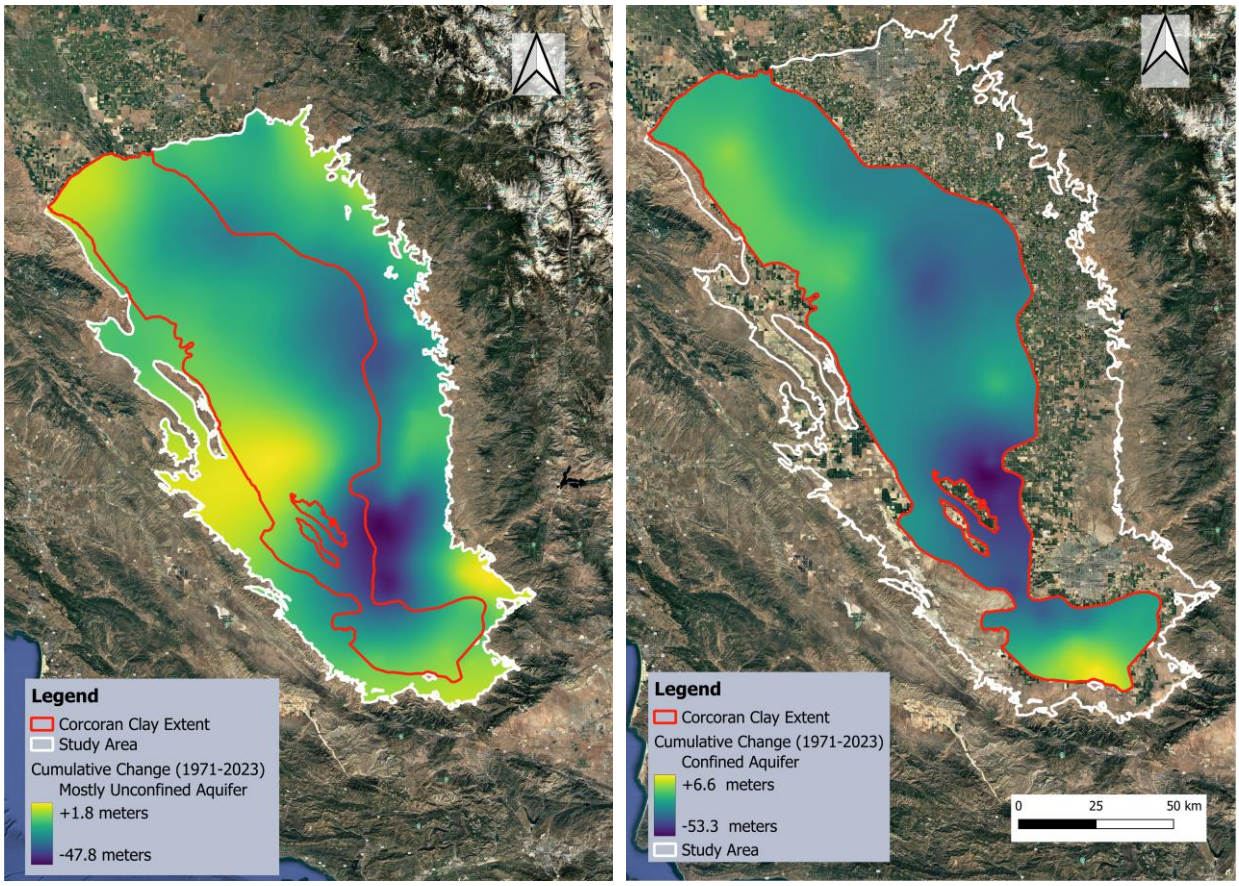

a **b**

Figure 7. Cumulative Groundwater Levels Change from 1971 to 2023 in Different Aquifer Layers;(a) Cumulative Change in Mostly Unconfined Aquifer and (b) Cumulative Change in Confined Aquifer. "+" sign implies increment, and "- "sign implies reduction in groundwater levels

The statistical metrics of absolute groundwater head over the 52-year time span showed an overall decreasing trend in groundwater (Figure 8; Table 1). The decline in this 52-year time span can be attributed to excessive groundwater extraction, compounded by drought conditions in the valley. We observed a very sharp decrease in groundwater head from 2012-2016. This can be linked to

the prolonged drought conditions in this period, recognized as one of the hottest droughts in California's recent history (California Department of Water Resources, 2021.; Mount et al., 2021). This caused farmers to rely more on groundwater for irrigation due to decreased precipitation. Moreover, aquifer recharge likely slowed down during this period, causing enhanced depletion. The groundwater head experienced a brief period of rise after the wet year in 2017, however it began to fall again in 2020 during the 2020–2022 drought period. We also observed a steep decrease in groundwater levels in other notable historical droughts including 2007-2009, 1987-1992 and 1976-1977 (California Department of Water Resource, 2021). The rise of the absolute head from 1982 to 1985 and 1995 to 1999 can be linked to the extended post drought recovery period after 1976-1977 and 1987-1992 droughts period respectively. These periods could have allowed continuous recharge and thus groundwater recovery.

Table 1. Reduction in groundwater levels (m) from 1971 to 2023 in Different Aquifer Layers

Type of Statistical Metrics	**Mostly Unconfined**	**Confined**
Mean	-16	-23
Median	-15	-24
Q1	-23	-30
Q3	-9	-15

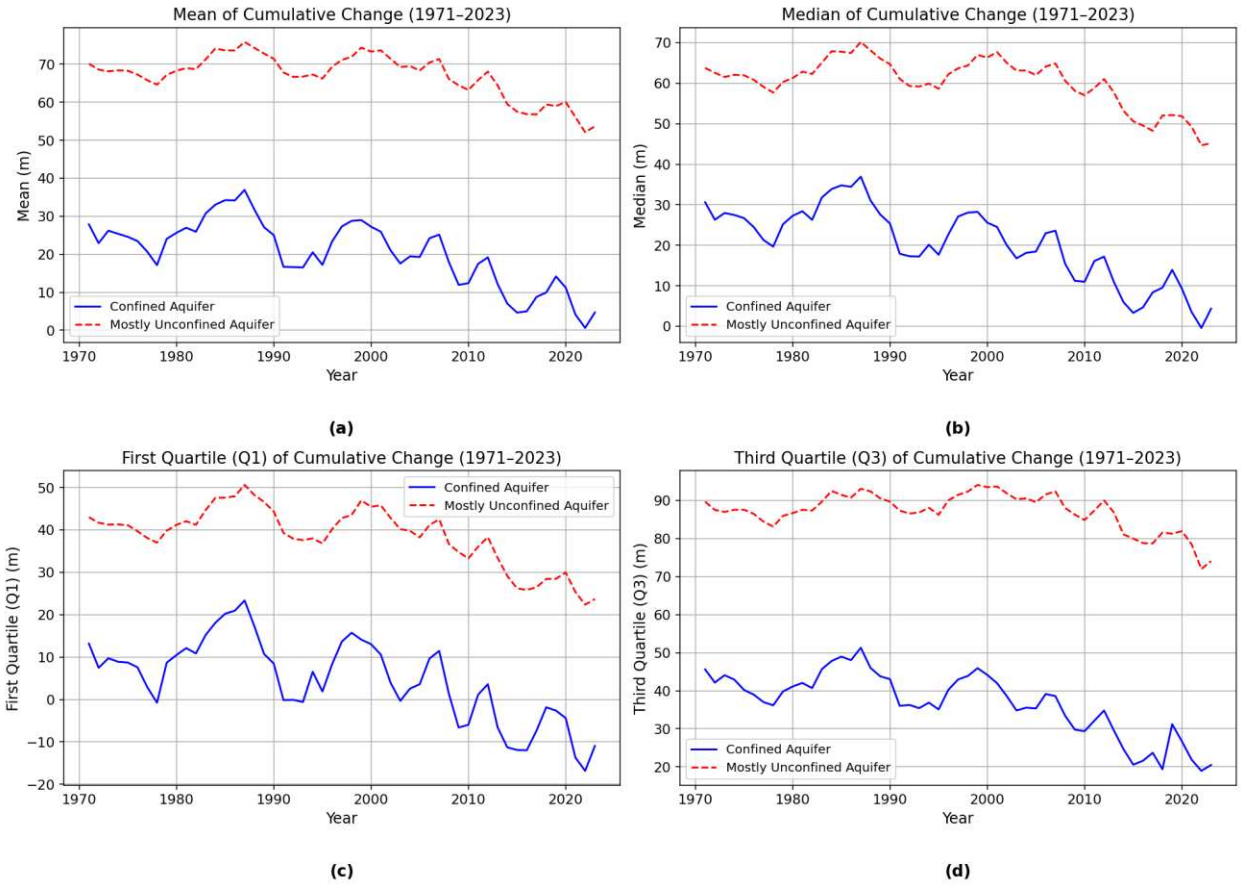

Figure 8. Statistical Metrics of Absolute Groundwater Head in the Study Area from 1971 to 2023- (a) Mean; (b) Median; (c) Q1 and (d) Q3

3.4 Comparison of the Combined Kriging-SBAS analysis with Conventional Interpolation Method

We compared the Combined Kriging SBAS (referred to as *"Kriging+SBAS"* hereafter) analysis with two conventional interpolation techniques: one where Kriging is applied to yearly groundwater levels (referred to as *"Only Kriging"* hereafter) and another where Kriging is performed on the yearly change in groundwater levels (referred to as *"Yearly Change Kriging"* hereafter). Wells from the CVHM-2 model, that had at least 10 years of groundwater levels measurements from 1971 to 2023 were selected (Faunt et al., 2022). 19 wells fulfilling this criterion were present in our study area, of which 14 belonged to mostly unconfined aquifers and

5 were present in the confined layer. The earliest year with groundwater level data for each well was determined. To compare the groundwater levels for all the previous years for which data were available, this was used as the reference point. The data from the reference year was then subtracted from the data available in the specified year to achieve this. For *"Only Kriging"* groundwater levels were estimated for each of the wells for each of the year using kriging interpolation. For each well, the reference year of the available data was identified and subtracted from the corresponding yearly records. Similarly, for "*Yearly Change Kriging*", Kriging was applied to interpolate yearly change in groundwater levels. Annual change starting from the reference year was considered to assess how the well levels have varied across all the years. Only interpolated temporal paired data that had corresponding records in the actual dataset were included in the analysis. Performance metrics namely, R-squared value(r^2), Root Mean Squared Error (RMSE), Mean Absolute Error (MAE), Mean Error (ME), and Normalized Mean Squared Error (NRMSE), were computed for all the three methods by comparing actual values with the predicted ones (Table 2). We observed that for both mostly unconfined and confined wells "*Kriging+SBAS*" outperformed other two methods. However, to more consistently show if the suggested approach provides better performance, validation over a greater number of wells with adequate high-quality data is required.

Table 2. Evaluation of Performance of the three different methods across two different Aquifers

Type	Method	r^2	RMSE (m)	MAE (m)	ME (m)	NRMSE
Mostly Unconfined	Kriging +SBAS	0.3	10.7	6.7	2.8	0.11
	Yearly Change Kriging	0.23	11.2	6.9	3.1	0.11
	Only Kriging	-0.09	13.4	8.1	2.4	0.13
Confined	Kriging +SBAS	0.46	6.1	4.8	2.9	0.1
	Yearly Change Kriging	0.42	6.3	5.2	3.3	0.11
	Only Kriging	-0.06	8.6	6.8	4	0.14

3.5 Groundwater Storage Loss from 2015 to 2023

We estimate that a total of 19.8 km^3 water was lost from the aquifer from 2015 to 2023. With 15.9 km^3 (80%) of the overall depletion, the mostly unconfined layer accounted for the majority of this loss. A negligible 0.01 km^3 (0.1%) of the depletion resulted from water expansion because of water's low compressibility, while 3.9 km^3 (20%) of storage loss was attributed to the compression of aquifer materials observed by InSAR. It is estimated that the total groundwater storage in the Central Valley ranges from 1,020 to 2,700 km^3 volume of freshwater at depths of 305 m to 1000 m (Kang and Jackson, 2016). Thus, our storage loss estimate corresponds to 0.7 to 1.9% of the total groundwater storage in the valley. Given that the study area covers only the one-third portion of the Central Valley, this depletion of aquifer is significant in just eight years of time.

Groundwater storage from the mostly unconfined section increased from 2017 to 2018, as water year 2017 was relatively wet compared to others, and then reduced during the drought. However,

loss from the aquifer matrix component consistently decreased with time in the 8-year period. This is because the fine-grained clay present in the aquifer matrix has low hydraulic conductivity, resulting in residual compaction due the previous stress history (Lees et al., 2022; Smith, 2023). In other words, the loss persisted because the deforming clay layers did not equilibrate to the drawdowns from the prior years (Smith & Li, 2021).

Liu et al., (2022), which used GRACE/FO data to estimate groundwater storage loss reported average loss of 4 km^3 of groundwater in the Tulare Basin from 2015 to 2022, while our estimate showed depletion of 25.6 km^3 in the same period in the study area. In the Central Valley, GRACE-based observations are significantly influenced by the adjacent mountains and foothills, leading to considerable different changes in water volume, which may cause leakage effects and thereby, underestimation of groundwater depletion in the valley (Stevens et al., 2025; Vasco et al., 2022). Likewise, we also observed notable differences in the storage loss estimation from CVHM-2 by Faunt et al., (2023) compared to Liu et al., (2022) for the entire Central Valley. Another study by Carlson et al., (2024) based on joint inversion of GNSS, GRACE and InSAR showed decline of 18.4 ± 1.7 km^3 of groundwater in the San Joaquin Valley/Tulare Basin from 8/2019 to 9/2021. Over the corresponding timeframe, Liu et al., (2022) computed the loss to be 3.6 km^3, while our study showed the drop of 12.5 km^3. Thus, change in storage estimates across the Central Valley vary widely based on the data sources and method used, highlighting the uncertainty in existing methods and the need for further research on how to best integrate in-situ and satellite datasets.

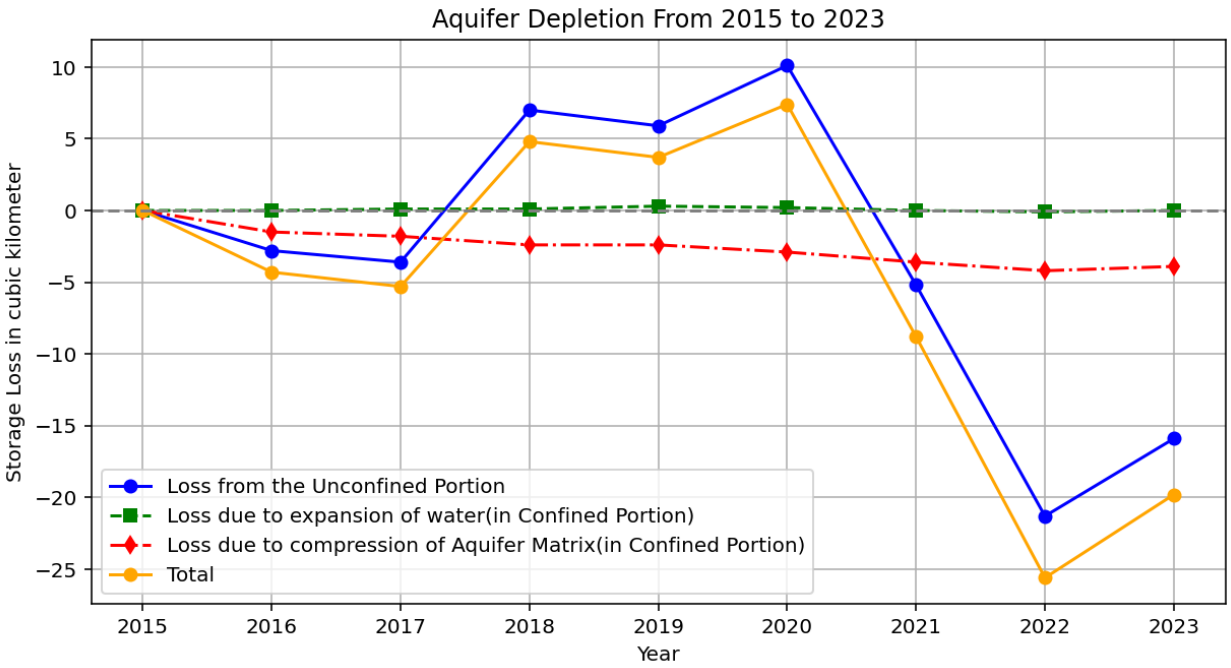

Figure 9. Aquifer Storage Loss from 2015 to 2023 from Confined and Mostly Unconfined Portion

4. CONCLUSIONS

We showed that groundwater levels in the study area is decreasing from 1971 to 2023, which was exacerbated by the prolonged drought conditions that occurred at various time intervals during this 52-year period. Our estimation of groundwater storage changes reveals that the storage depletion is primarily attributed to loss from the upper unconfined aquifer and followed by the compression of fine grained and coarse-grained materials.

In areas like San Joaquin Valley, where groundwater is depleting at an alarming rate, it is essential to correctly monitor groundwater levels. We have demonstrated a novel method that first classifies the wells in the valley to the respective aquifer system and then interpolates groundwater level changes. Thus, we present a new dataset of groundwater level declines in the southern San Joaquin Valley that has improved spatiotemporal density and accuracy. This can lead to better and accurate estimation of groundwater storage change and groundwater modeling in this region. Likewise, the described method can be a promising technique to effectively estimate groundwater levels in other regions across broad spatial and temporal scales. Future studies could include estimating groundwater scales at a finer spatial and temporal resolution, as well as enhancing storage coefficient parameter estimation for more refined storage loss estimates.

5. REFERENCES

Akhter, T., Naz, M., Salehin, M., Arif, S. T., Hoque, S. F., Hope, R., & Rahman, M. R. (2023). Hydrogeologic Constraints for Drinking Water Security in Southwest Coastal Bangladesh: Implications for Sustainable Development Goal 6.1. *Water (Switzerland)*, *15*(13). https://doi.org/10.3390/w15132333

Berardino, P., Fornaro, G., Lanari, R., & Sansosti, E. (2002). A new algorithm for surface deformation monitoring based on small baseline differential SAR interferograms. *IEEE Transactions on Geoscience and Remote Sensing*, *40*(11), 2375–2383. https://doi.org/10.1109/TGRS.2002.803792

Bland, A. (2023, February 7). *Ground zero: Rain brings little relief to California's depleted groundwater*. https://calmatters.org/environment/water/2023/02/california-depleted-groundwater-storms/

California Department of Food and Agriculture. (2022). *California Agricultural Statistics Review 2021–2022*. Sacramento, CA. Retrieved from https://www.cdfa.ca.gov/Statistics/PDFs/2022_Ag_Stats_Review.pdf

California Department of Water Resources (DWR), U. S. B. of R. (2016). Final Environmental Impact Report / Environmental Impact Statement for the Bay Delta Conservation Plan / California WaterFix: Appendix 7A – Groundwater Model Documentation. https://www.waterboards.ca.gov/waterrights/water_issues/programs/bay_delta/california_waterfix/exhibits/exhibit102/docs/vol1/Final_EIR-EIS_Appendix_7A_-_Groundwater_Model_Documentation.pdf

California Natural Resources Agency Open Data. (2025). *Periodic Groundwater Level Measurements - Dataset - California Natural Resources Agency Open Data*. https://data.cnra.ca.gov/dataset/periodic-groundwater-level-measurements

California Water Library. (2025). https://cawaterlibrary.net/hydrological-region/tulare-lake/

Carlson, G., Werth, S., & Shirzaei, M. (2024). A novel hybrid GNSS, GRACE, and InSAR joint inversion approach to constrain water loss during a record-setting drought in California. *Remote Sensing of Environment*, *311*, 114303.

Croft, M. G. (1972). Subsurface geology of the late Tertiary and Quaternary water-bearing deposits of the southern part of the San Joaquin Valley, California. https://doi.org/10.3133/wsp1999H

Drought. (2021). https://water.ca.gov/drought

Droughts in California - Public Policy Institute of California. (2021). https://www.ppic.org/publication/droughts-in-california/

Dry Well Reporting System. (2025). https://mydrywatersupply.water.ca.gov/report/publicpage

Errors in groundwater level measurement | British Geological Survey (BGS). (n.d.). Retrieved August 25, 2024, from https://www2.bgs.ac.uk/groundwater/datainfo/levels/measuring_errors.html

Evans, S. W., Jones, N. L., Williams, G. P., Ames, D. P., & Nelson, E. J. (2020). Groundwater Level Mapping Tool: An open source web application for assessing groundwater sustainability. *Environmental Modelling & Software*, *131*, 104782. https://doi.org/10.1016/j.envsoft.2020.104782

Faunt, C. C., Hanson, R. T., Belitz, K., Schmid, W., Predmore, S. P., Rewis, D. L., & McPherson, K. (2009). Groundwater availability of the Central Valley Aquifer, California. U.S. Geological Survey. https://pubs.usgs.gov/pp/1766/PP_1766.pdf

Faunt, C. C., Sneed, M., Traum, J., & Brandt, J. T. (2016). Water availability and land subsidence in the Central Valley, California, USA. *Hydrogeology Journal*, *24*(3), 675–684. https://doi.org/10.1007/s10040-015-1339-x

Faunt, C. C., Stamos-Pfeiffer, C. L., Brandt, J. T., Sneed, M., & Boyce, S. E. (2022). Central Valley Hydrologic Model version 2 (CVHM2): Observation Data (Groundwater Level, Streamflow, Subsidence) (ver. 2.2, May 2024). U.S. Geological Survey Data Release.

Faunt, C. C., Traum, J. A., Boyce, S. E., Seymour, W. A., Jachens, E. R., Brandt, J. T., ... & Marcelli, M. F. (2024). Groundwater sustainability and land subsidence in California's Central Valley. *Water*, *16*(8), 1189.

Freeze, R. A., & Cherry, J. A. (1979). *GROUNDWATER* (First). Prentice-Hall, Inc. https://fc79.gw-project.org/english/

Galloway, D., & Riley, F. S. (1999). San Joaquin Valley: California Largest Human Alteration of the Earth's Surface. Land Subsidence in the United States. https://pubs.usgs.gov/circ/circ1182/pdf/06SanJoaquinValley.pdf

Hanak, E., Jezdimirovic, J., Escriva-Bou, A., & Ayres, A. (2020). A Review of Groundwater Sustainability Plans in the San Joaquin Valley.

Hasan, M. F., Smith, R., Vajedian, S., Pommerenke, R., & Majumdar, S. (2023). Global land subsidence mapping reveals widespread loss of aquifer storage capacity. *Nature Communications*, *14*(1). https://doi.org/10.1038/s41467-023-41933-z

Jasechko, S., Seybold, H., Perrone, D., Fan, Y., Shamsudduha, M., Taylor, R. G., Fallatah, O., & Kirchner, J. W. (2024). Rapid groundwater decline and some cases of recovery in aquifers globally. *Nature*, *625*(7996), 715–721. https://doi.org/10.1038/s41586-023-06879-8

Jia, X., Hou, D., Wang, L., O'Connor, D., & Luo, J. (2020). The development of groundwater research in the past 40 years: A burgeoning trend in groundwater depletion and sustainable management. *Journal of Hydrology*, *587*. https://doi.org/10.1016/j.jhydrol.2020.125006

Júnez-Ferreira, H. E., Hernández-Hernández, M. A., Herrera, G. S., González-Trinidad, J., Cappello, C., Maggio, S., & De Iaco, S. (2023). Assessment of changes in regional groundwater levels through spatio-temporal kriging: application to the southern Basin of Mexico aquifer system. *Hydrogeology Journal*, *31*(6), 1405–1423. https://doi.org/10.1007/s10040-023-02681-y

Kang, M., & Jackson, R. B. (2016). Salinity of deep groundwater in California: Water quantity, quality, and protection. *Proceedings of the National Academy of Sciences*, *113*(28), 7768-7773.

Lees, M., & Knight, R. (2023). Integrating shallow head measurements and InSAR data to quantify groundwater-storage change in San Joaquin Valley, California (USA). *Hydrogeology Journal*, *31*(8), 2041–2060. https://doi.org/10.1007/s10040-023-02705-7

Lees, M., Knight, R., & Smith, R. (2022). Development and Application of a 1D Compaction Model to Understand 65 Years of Subsidence in the San Joaquin Valley. *Water Resources Research*, *58*(6). https://doi.org/10.1029/2021WR031390

Levy, Z. F., Jurgens, B. C., Burow, K. R., Voss, S. A., Faulkner, K. E., Arroyo-Lopez, J. A., & Fram, M. S. (2021). Critical Aquifer Overdraft Accelerates Degradation of Groundwater Quality in California's Central Valley During Drought. *Geophysical Research Letters*, *48*(17). https://doi.org/10.1029/2021GL094398

Li, S., Xu, W., & Li, Z. (2022). Review of the SBAS InSAR Time-series algorithms, applications, and challenges. *Geodesy and Geodynamics*, *13*(2), 114–126. https://doi.org/10.1016/j.geog.2021.09.007

Liu, P. W., Famiglietti, J. S., Purdy, A. J., Adams, K. H., McEvoy, A. L., Reager, J. T., Bindlish, R., Wiese, D. N., David, C. H., & Rodell, M. (2022). Groundwater depletion in California's Central Valley accelerates during megadrought. *Nature Communications*, *13*(1). https://doi.org/10.1038/s41467-022-35582-x

Masoudi, P., Faucheux, C., & Binet, H. (2024). Mapping Groundwater Level by Geostatistical Methods: Ordinary Versus Universal Kriging; Alongside a Discussion on Neighbourhood.

85th EAGE Annual Conference & Exhibition (Including the Workshop Programme), *2024*, 1–5.

Mayzelle, M. M., Viers, J. H., Medellín-Azuara, J., & Harter, T. (2015). Economic feasibility of irrigated agricultural land use buffers to reduce groundwater nitrate in rural drinking: Water sources. Water (Switzerland), 7(1), 12–37. https://doi.org/10.3390/w7010012

Neely, W. R., Knight, R., Kang, S., & Goebel, M. (2024). Exploring the InSAR signature associated with river-sourced recharge in California's San Joaquin Valley. *Environmental Research Letters*, *19*(7). https://doi.org/10.1088/1748-9326/ad5855

Ojha, C., Werth, S., & Shirzaei, M. (2019). Groundwater Loss and Aquifer System Compaction in San Joaquin Valley During 2012–2015 Drought. *Journal of Geophysical Research: Solid Earth*, *124*(3), 3127–3143. https://doi.org/10.1029/2018JB016083

Page, R. W. (1986). Geology of the Fresh Ground-Water Basin of the Central Valley, California, with Texture Maps and Sections REGIONAL AQUIFER-SYSTEM ANALYSIS.

Peterson, T. J., & Western, A. W. (2018). Statistical Interpolation of Groundwater Hydrographs. *Water Resources Research*, *54*(7), 4663–4680. https://doi.org/10.1029/2017WR021838

Phillips, S. P., Green, C. T., Burow, K. R., Shelton, J. L., & Rewis, D. L. (2007). Simulation of Multiscale Ground-Water Flow in Part of the Northeastern San Joaquin Valley, California.

Poland, J. F., Lofgren, B. E., Ireland, R. L., & Pugh, R. G. (1975). Land Subsidence in the San Joaquin Valley, California, As of 1972. In *U.S. Geological Survey Professional Paper 437-H*. https://pubs.usgs.gov/pp/0437h/report.pdf

Pradhan, A., Adams, K. H., Chandrasekaran, V., Liu, Z., Reager, J. T., Stuart, A. M., & Turmon, M. J. (2024). Modeling Groundwater Levels in California's Central Valley by Hierarchical Gaussian Process and Neural Network Regression. *Journal of Geophysical Research: Machine Learning and Computation*, *1*(4). https://doi.org/10.1029/2024JH000322

Retike, I., Bikše, J., Kalvāns, A., Dēliņa, A., Avotniece, Z., Zaadnoordijk, W. J., Jemeljanova, M., Popovs, K., Babre, A., Zelenkevičs, A., & Baikovs, A. (2022). Rescue of groundwater level time series: How to visually identify and treat errors. *Journal of Hydrology*, *605*. https://doi.org/10.1016/j.jhydrol.2021.127294

Ruybal, C. J., Hogue, T. S., & McCray, J. E. (2019). Evaluation of groundwater levels in the Arapahoe aquifer using spatiotemporal regression kriging. *Water Resources Research*, *55*(4), 2820-2837.

Smith, R. (2023). Aquifer Stress History Contributes to Historic Shift in Subsidence in the San Joaquin Valley, California. *Water Resources Research*, *59*(11). https://doi.org/10.1029/2023WR035804

Smith, R. G., Knight, R., Chen, J., Reeves, J. A., Zebker, H. A., Farr, T., & Liu, Z. (2017). Estimating the permanent loss of groundwater storage in the southern San Joaquin Valley, California. *Water Resources Research*, *53*(3), 2133–2148. https://doi.org/10.1002/2016WR019861

Smith, R., & Knight, R. (2019). Modeling Land Subsidence Using InSAR and Airborne Electromagnetic Data. *Water Resources Research*, *55*(4), 2801–2819. https://doi.org/10.1029/2018WR024185

Smith, R., Knight, R., & Fendorf, S. (2018). Overpumping leads to California groundwater arsenic threat. *Nature Communications*, *9*(1). https://doi.org/10.1038/s41467-018-04475-3

Smith, R., & Li, J. (2021). Modeling elastic and inelastic pumping-induced deformation with incomplete water level records in Parowan Valley, Utah. *Journal of Hydrology*, *601*. https://doi.org/10.1016/j.jhydrol.2021.126654

Snyder, D. T. (2008). Estimated Depth to Ground Water and Configuration of the Water Table in the Portland, Oregon Area: : U.S. Geological Survey Scientific Investigations Report 2008–5059.

Stevens, M. D., Ramirez, S. G., Martin, E. M. H., Jones, N. L., Williams, G. P., Adams, K. H., Ames, D. P., & Pulla, S. T. (2025). Groundwater storage loss in the central valley analysis using a novel method based on in situ data compared to GRACE-derived data. *Environmental Modelling and Software*, *186*. https://doi.org/10.1016/j.envsoft.2025.106368

Tao, H., Hameed, M. M., Marhoon, H. A., Zounemat-Kermani, M., Heddam, S., Sungwon, K., Sulaiman, S. O., Tan, M. L., Sa'adi, Z., Mehr, A. D., Allawi, M. F., Abba, S. I., Zain, J. M., Falah, M. W., Jamei, M., Bokde, N. D., Bayatvarkeshi, M., Al-Mukhtar, M., Bhagat, S. K., … Yaseen, Z. M. (2022). Groundwater level prediction using machine learning models: A comprehensive review. In *Neurocomputing* (Vol. 489, pp. 271–308). Elsevier B.V. https://doi.org/10.1016/j.neucom.2022.03.014

Taylor, C. J., & Alley, W. M. (2001). Ground-Water-Level Monitoring and the Importance of Long-Term Water-Level Data.

Tre Altamira. (2024). https://data.ca.gov/dataset/tre-altamira-insar-subsidence-data

Tulare Basin | USGS California Water Science Center. (2025). https://ca.water.usgs.gov/projects/central-valley/tulare-basin.html

United Nations. (2022). *The United Nations World Water Development Report 2022: GROUNDWATER Making the invisible visible*. United Nations Educational, Scientific and

Cultural Organization. https://www.unwater.org/publications/un-world-water-development-report-2022

U.S. Geological Survey. (2023). Contours of Corcoran Clay Thickness in feet by Page (1986) for the Central Valley Hydrologic Model (CVHM) | USGS Science Data Catalog. https://doi.org/https://doi.org/10.5066/P9O6FJ24

Vasco, D. W., Kim, K. H., Farr, T. G., Reager, J. T., Bekaert, D., Sangha, S. S., ... & Beaudoing, H. K. (2022). Using Sentinel-1 and GRACE satellite data to monitor the hydrological variations within the Tulare Basin, California. *Scientific Reports*, *12*(1), 3867.

Visser, M. A., Kumetat, G., & Scott, G. (2024). Drought, water management, and agricultural livelihoods: Understanding human-ecological system management and livelihood strategies of farmer's in rural California. *Journal of Rural Studies*, *109*. https://doi.org/10.1016/j.jrurstud.2024.103339

Yu, Z., Zhang, G., Huang, G., Cheng, C., Zhang, Z., & Zhang, C. (2024). SSBAS-InSAR: A Spatially Constrained Small Baseline Subset InSAR Technique for Refined Time-Series Deformation Monitoring. *Remote Sensing*, *16*(18). https://doi.org/10.3390/rs16183515